

Electromagnetic shielding effectiveness of lightweight and flexible ultrathin shungite plates

Igor V. Antonets^{a, **}, Yevgeny A. Golubev^{b, *}, Vladimir I. Shcheglov^c, Shiyong Sun^d

^a Department of Radiophysics, Syktyvkar State University, Syktyvkar, 167000, Russia

^b Institute of Geology of Komi SC, Russian Academy of Sciences, Syktyvkar, 167982, Russia

^c Institute of Radio Engineering and Electronics, Russian Academy of Sciences, Moscow, 125009, Russia

^d Southwest University of Science and Technology, Mianyang, 621010, PR China

ARTICLE INFO

Keywords:

Graphene-containing shungite carbon
Ultrathin and flexible shungite shielding materials
Microwave radiation
Reflecting and absorbed effectiveness
Dynamic conductivity

ABSTRACT

Carbon-containing shielding materials, especially with absorbing properties, received a lot of attention from the scientific community as having flexibility, lightness and corrosion resistance. Reducing the thickness of such materials (usually a few millimeters) is also an urgent task. In this paper, we offered results of studying the reflective and absorbing properties of shielding materials from natural graphene-containing shungite. Flexible shungite plates with a thickness of 10–20 μm showed good reflection and absorption similar shielding performance to a thicker 2–3 mm synthetic polymer/carbon based composites. Such characteristics are associated with the fact that shungites are unique natural composites with a conductive carbon matrix and micro-sized dielectric mineral inclusions. Shungite could be considered as a raw to manufacture shielding materials, and as a model for more complete understanding of interaction of radiation with graphene-containing conducting solids in order to improve the shielding performances.

1. Introduction

The design of microwave electronic devices and increasing their power makes the development of new materials relevant for reducing noise and ensuring electromagnetic compatibility. Absorbing materials have received a lot of attention, in particular, due to the negative effect of the reflections of electromagnetic radiation inside buildings or technical devices. During the last decades, a large amount of studies have been focused on the design of shielding absorption materials, based on composite polymeric materials due to their lightness, low cost, easy shaping, etc. [1–3].

Electrically conductive polymer composites received much attention compared to conventional shielding metallic materials [1,4–6] because of their low mass, resistance to corrosion, and flexibility. Flexible shield technology is of great interest to the electronics industry for portable applications because the flexible substrate can be rolled and bent to fit a limited space [3].

Flexible shielding materials are mainly produced on the basis of dielectric polymer matrices that are filled with carbon materials (nanotubes, fullerenes, nanoparticles with graphite-like structure). This

leads to the fact that the amount of filler should be sufficient to exceed the percolation threshold, and the thickness of such materials for effective shielding is a few millimeters. If the systems are made on the basis of conductive polymer and carbon matrices, this leads to a good reflection efficiency, while such systems have weak absorbing properties. For the highest absorption efficiency, honeycomb and foam structures are used [1]. The efficiency of their absorption reaches 70–90%, however, the thickness of such materials is also several millimeters. Reducing the thickness of shielding coatings is a promising task.

To solve some of the above-mentioned tasks, the shungites from Karelia are promising natural composite materials. Glass-like carbon with packs of disoriented nano-sized graphene layers and micro-sized quartz crystals are uniformly distributed in them. The carbon content varies from close to zero to almost 100%, which is favorable to study of influence of carbon content on the shielding properties, and accordingly, to vary these properties. Analysis of scientific and technical data suggests the promise of shungite-based materials in the manufacture of shielding materials and protective coatings in metallurgy, building, medicine, etc. [7–10]. Shungites have unique properties, including improved strength and durability, high chemical stability and electrical

* Corresponding author.

** Corresponding author.

E-mail addresses: aiv@mail.ru (I.V. Antonets), yevgenyGolubev74@mail.ru (Y.A. Golubev), shysun@168.com (S. Sun).

<https://doi.org/10.1016/j.cap.2021.06.008>

Received 7 November 2020; Received in revised form 8 June 2021; Accepted 19 June 2021

Available online 30 June 2021

1567-1739/© 2021 Korean Physical Society. Published by Elsevier B.V. All rights reserved.

conductivity, fire resistance. The especial structure and potential for technological applications continue to stimulate interest in shungite carbon [11–13]. Shielding materials like shungite will have not only a high shielding efficiency and a wide absorption band, but will be also light, very thin and cost effective. Here we proposed to consider the shungites of Karelia as a model system of shielding material with reflective and absorbing properties based on a highly conductive graphene-containing carbon matrix and microscale dielectric filler.

Shungites are carbon-containing Precambrian rocks in Karelia, Russia [7,14]. “Pure” shungite carbon consists of C_{org} (~90–95%) and contains H (~1%), N (~0.8%), S (~0.4%), O (~2.4%) [7,14]. The structure of shungite carbon is referred to as poorly ordered graphite [15]; amorphous carbon [16]; natural metastable non-graphitized carbon with fullerene-like multilayer globules [17]; aggregate of stacks of graphene layers [18,19]; and glassy carbon [20]. In general, shungite is a natural composite of carbon nanostructures and turbostratic carbon with a variety of mineral inclusions (pyrite, quartz, sericite, chlorite). The shungite nanoscale structure is deformed graphene planes folded into stacks [21]. Technologically promising electromagnetic properties of shungites are associated with such structural features [8–10].

The information about the microwave properties of shungites is contradictory. The shungite-containing samples in different fragments of the frequency range from 100 kHz to 40 GHz presented increasing reflection efficiency with frequency [22,23], and the absence of this increase [24,25]. These differences can result from different techniques for samples preparation with powdered shungite and shungite-containing composites.

In [26], a significant excess of the dynamic conductivity of shungite plates with a thickness of 10–20 μm over the static conductivity in the range of carbon contents of 5–30% in the 8–12 GHz microwave range was revealed. In this regard, the characteristic of reflection and absorption of microwave radiation by shungites, as well as the explanation of their dependence on carbon content, are of interest as to the characteristics of shielding systems “conducting matrix - dielectric filler” for technological applications. Here we will talk about the effect of carbon content on the reflective, transmitted and absorbing properties of thin flexible shungite plates in the 26–38 GHz microwave range.

2. Material and methods

2.1. Samples preparation

Samples for the study were selected to uniformly cover the range of carbon contents (from 3 to 97 at. %) from large deposits (Maxovo, Zazhogino, Shunga, and Lebeshchina) of carbonaceous substances in Karelia, Russia [7,14].

Plate manufacturing technology was described in Ref. [26]. Initial shungite plates (2 mm in thickness and about 2.5×1.5 cm in size) were cut from pieces of rocks (Fig. 1). These plates were glued onto standard laboratory glass using Canadian balsam and polished to the desired thickness of 10–20 μm . After that, a thin shungite plate was removed from the glass using adhesive tape.

The remains of a piece of rock were ground into powder and used to

measure the carbon content (in weight percent) using AN-7529M express analyzer by automatic coulometric titration on to the pH value. Previously carbonate carbon was removed by hydrochloric acid. After that, it was recalculated into atomic content.

The optimal thickness of shungite plates to study the reflecting and absorbing properties was previously selected from the plates with thickness of 0.5 mm; 0.3 mm; 0.1 mm; ~50 μm and ~15 μm . The studied plates in the thickness range of 0.5 mm–50 μm reflect 100% of the incident radiation. In addition, plates with a thickness of more than 0.1 mm are brittle and break when bent. The shungite plate ~15 μm thick reflects, transmits and absorbs electromagnetic radiation. In addition, this plate was very flexible. Therefore, such a thickness of the plates was chosen for our experiments.

2.2. Plates thickness measurement

The plate thicknesses were determined using Tescan MIRA3 (Czech Republic) scanning electron microscope (SEM). The measurements were carried out on cut fragments of plates with the length of about 1 cm. For this, an adhesive tape with a shungite plate was glued onto a MoS_2 cubic crystal so that the plate protruded beyond the upper edge of the crystal. This protrusion of the scotch tape was tearing off with tweezers, and then the crystal was placed in the microscope chamber with the chipped end of the shungite plate up. The chipped end thickness of the plate was measured at 15 points using microscope software (Fig. 2). The points for thickness measurement were chosen equidistantly along the entire length of the plate fragment.

2.3. Measurements of the reflection and transmission coefficients

The reflection and transmission coefficients of the microwave signal from shungite plates at a normal wave incidence in the frequency range 26–38 GHz were measured. The shungite plate was placed in a rectangular waveguide 7×3 mm in size and completely covered the whole section of the waveguide. The waveguide was connected to a panoramic waveguide microwave spectrometer including a swept-frequency oscillator combined with an indicator of the standing wave ratio with an attenuation module, and a waveguide set of reflectometers (Fig. 3). The reflection and transmission coefficients were measured from the power.

The reflection coefficient R was determined as:

$$R = \left(\frac{K - 1}{K + 1} \right)^2 = \frac{W_{\text{refl}}}{W_{\text{inc}}} \quad (1)$$

where K is the standing-wave ratio (determined directly on the indicator scale), W_{inc} and W_{refl} are the power of the incident and reflected waves, respectively.

The transmission coefficient was determined similarly, by means of standing-wave ratio values taken from the indicator scale and characterizing the attenuation of the signal passing through the sample.

The transmission coefficient was calculated by:

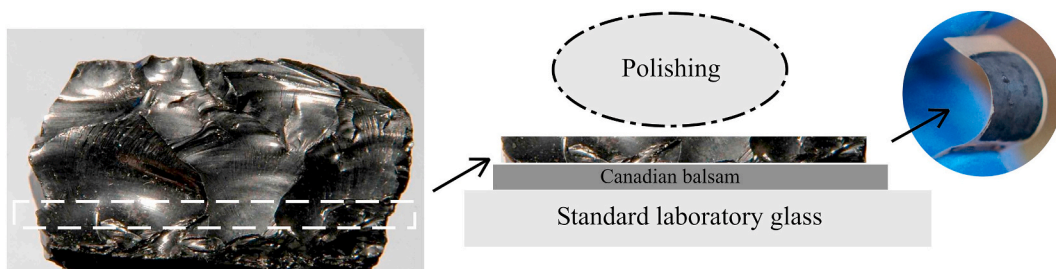


Fig. 1. Preparation process of shungite plates.

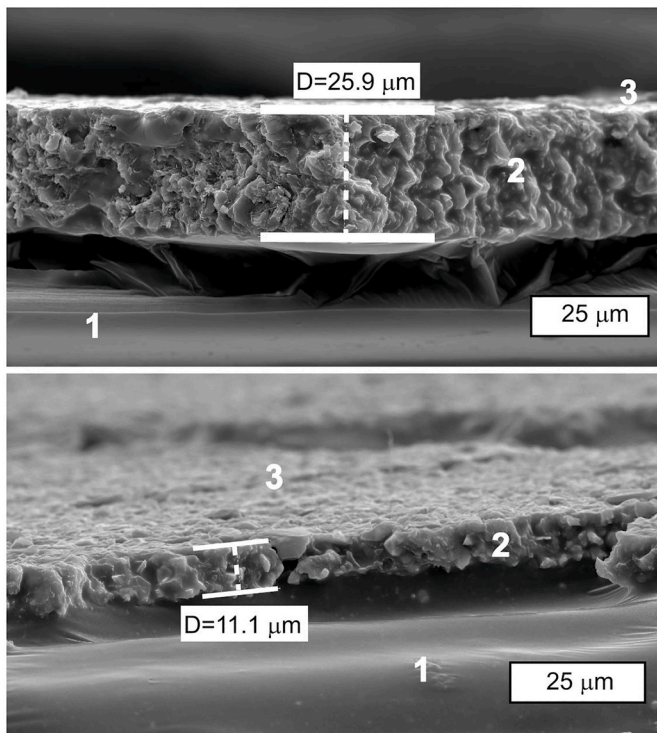


Fig. 2. Examples of measuring the thickness of a shungite plate using electron microscopic images of the cleaved end (samples ShSh5 (a) and ShM3 (b)). 1 – adhesive tape surface; 2 – shungite plate chipped end; 3 – plate surface.

$$T = \left(\frac{K - 1}{K + 1} \right)^2 = \left(\frac{E_{trans}}{E_{ins}} \right)^2 \tag{2}$$

where K is the standing-wave ratio, E_{ins} and E_{trans} are the power of the incident and transmitted waves, respectively.

According to the reflection (R) and transmission (T) coefficients, the absorption coefficient of a shungite plate (A) was determined as:

$$A = 1 - R - T. \tag{3}$$

2.4. Measurements of static conductivity

Samples for static conductivity measuring were fabricated as plane-parallel rectangular plates with sizes of about 1×1 cm and a thickness of about 0.5 mm. Electrical conductivity was measured using V7-27A resistivity meter (Tetron, Russia) connected with a four-pin probe from copper wires. The inter-pin spacing was 2 mm and the pin diameter was 0.55 mm. The pin tips were covered with a silver paste to improve contact with the sample surface.

3. Results

3.1. Carbon content, conductivity and thickness of shungite plates

The studied shungite samples almost evenly cover the range of carbon content from 2 to 97 at. % (Table 1). The static conductivity varies from tens to several thousand S/m and is clearly dependent on the carbon content (Table 1). The thickness of the plates mainly varies in a narrow range of 11–15 μm.

The surface morphology was studied by scanning electron microscopy (SEM). The microstructure of shungite plates withstands multiple bends. The ability of the plates to withstand multiple bends without

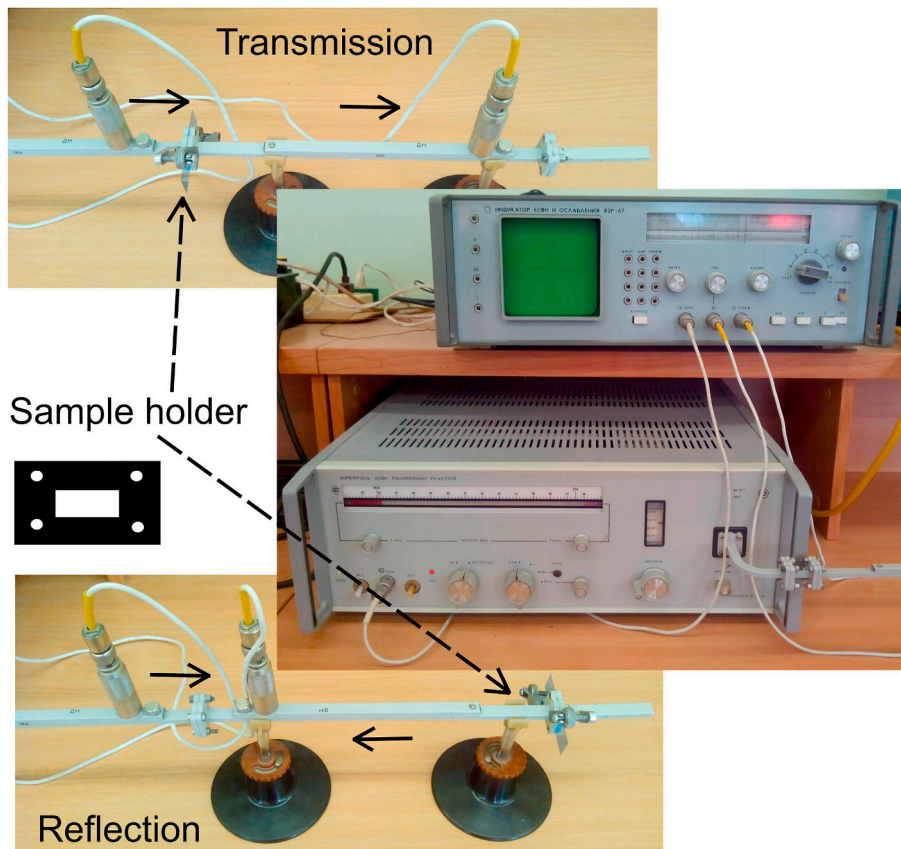


Fig. 3. Instrumental set-up for measuring the reflected (bottom) and transmitted (top) radiation.

Table 1
Carbon content (weight and atomic %) and thickness of shungite plates.

Sample code	Locality (deposit)	C content, at%	Thickness, μm
ShSh1	Shunga	97	12 ± 1
ShSh2	Shunga	73	15 ± 1
ShL2	Lebeshchina	64	12 ± 2
M59	Maxovo	57	14 ± 1
M58	Maxovo	53	8 ± 1
ShL2a	Lebeshchina	49	15 ± 2
ShZ3	Zazhogino	47	12 ± 2
ShM3	Maxovo	41	11 ± 1
ShKG3	Chebolaksha	37	14 ± 1
ShCh3	Chebolaksha	34	11 ± 2
M29	Maxovo	25	13 ± 1
M30	Maxovo	23	15 ± 2
M25	Maxovo	17	13 ± 3
ShSh5	Shunga	5	19 ± 2
ShN5	Nigozero	2	15 ± 1

surface cracking increases with increasing carbon content (Fig. 4).

3.2. Microwave properties in the range 26–38 GHz

Fig. 5a shows the dependence of the reflection coefficient of the microwave signal R on the carbon concentration C in the frequency range $f = 26$ –38 GHz. The values of the reflection coefficient at a frequency of 31 GHz are almost always located between the values of the reflection coefficient at frequencies of 29 and 33 GHz, therefore, an approximation was performed according to the experimental points at a frequency of 31 GHz according to the following equation [26,27]:

$$y(x) = \frac{A_1 - A_2}{1 - \exp\left(\frac{x-x_0}{dx}\right)} + A_2 \quad (4)$$

where, $y(x) = R(C)$; $A_1 = -6.74$; $A_2 = 1.00$; $x_0 = -70.96$; $dx = 37.22$.

In this equation, A_1 and A_2 are the constants that determine the minimum (initial) and maximum (final) value of the function $y(x)$ and are dependent on the substance characteristics; x_0 is the carbon content at which the function $y(x)$ reaches its mean value between A_1 and A_2 . A_1 at $x \rightarrow 0$ (i.e., at $C \rightarrow 0$) is determined by the characteristics of substrate.

The reflection coefficient R for shungites with a carbon content of up to ~35% gradual increases (Fig. 5). When the carbon content is above ~35%, the reflection coefficient changes less dramatically. For low-carbon samples with C content up to about 35%, a significant scatter of points in frequency is observed. For samples with carbon content higher than 50%, the fluctuations of $R(f)$ are gradually smoothed out, and the scatter of points in frequency becomes much smaller. For high-carbon samples ($C > 60\%$), the reflection coefficient changes only

slightly with frequency, and deviations from the average value of frequency reflection are no more than 5%.

Fig. 5b shows the dependence of the transmission coefficient of microwave radiation on the carbon content. Experimental points at a frequency of 31 GHz are approximated with equation:

$$y(x) = y_0 + B \exp\left(-\frac{x}{t}\right), \quad (5)$$

where $y(x) = T(C)$; $y_0 = 0$; $B = 1.00$; $t = 7.90$.

It can be seen that already with a carbon content of more than 10%, the transmission becomes small (10% or less), and with a carbon content of more than 40%, the transmission is extremely small and within the measurement error of the device (about 1–3%).

The absorption of electromagnetic radiation is maximal ($A = 0.40$ –0.45) in the range of carbon contents of 5–35% (Fig. 5c). This range of concentrations accounts for the main increase in the reflection coefficient and the decrease in the transmission coefficient. When the carbon content exceeds 40%, the absorption decreases by two to three times due to increasing reflection. With a carbon content of less than 5%, almost all radiation transmits through the plate.

Shungite plates 10–20 μm in thick with a carbon content of over 35% completely shield the electromagnetic radiation. At the same time, in samples with a carbon content of more than 60%, shielding occurs due to reflection of electromagnetic radiation.

Since the reflection also increases with the carbon content and occurs before the absorption, there is a lower proportion of the radiation left for absorption. The proportion of the power absorbed by the materials reaches a maximum before decreasing at a high electrical conductivity. It actually never surpasses 50% for our samples. Indeed, though the absorption capacity is improved, there is a lower proportion of the radiation left for absorption after the intensive reflection associated to the high conductivity.

In the range of carbon contents of 35–60%, about 70–80% of the microwave radiation is already reflected; the rest is absorbed in the sample. With the carbon content of 17–35%, the shielding efficiency is about 80–90%, while the absorption and reflection efficiency is about the same. For a sample with a carbon content of 25%, the shielding efficiency is almost 100% with high absorption efficiency (30%). The shielding efficiency decreases to 5% when the carbon content is less than 2%.

3.3. The theoretical prediction of reflection, transmission and absorption

A theoretical estimate of the reflection (R), transmission (T) and absorption (A) coefficients of a thin layer of shungite depending on the carbon concentration was carried out by the averaging method based on

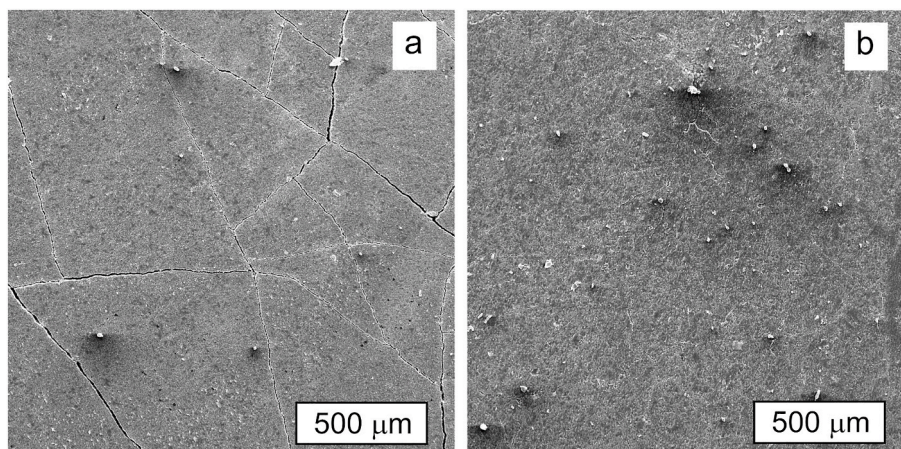


Fig. 4. SEM image of the plates of samples ShKG3 (a) and ShL2 (b) after a cycle from 100 flexions/extensions.

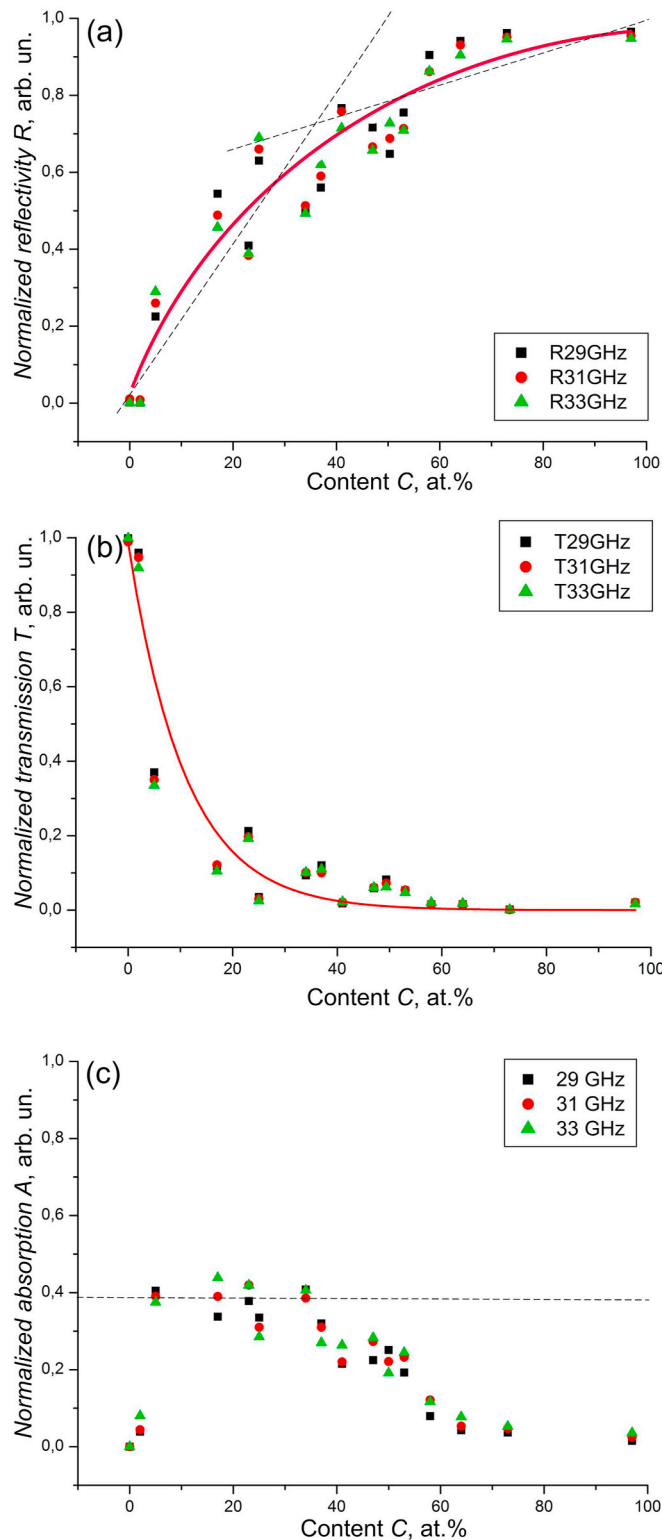


Fig. 5. The dependence of the reflection (a), transmission (b) and absorption (c) of electromagnetic radiation on the carbon concentration of shungite plates in the frequency range 26–38 GHz. Approximation (red line in (a) and (b)) is made at a frequency of 31 GHz. The dotted lines on (a) mark the approximations of the two parts of the curve (from zero to 40% and from 40% to 97%). (For interpretation of the references to colour in this figure legend, the reader is referred to the Web version of this article.)

the integral form of the Maxwell equations [28]. We considered a model where a plane electromagnetic wave fell normally on a thin layer of conductive (carbon-containing) material with a thickness d , the static conductivity of which depended on the carbon content $\sigma(C)$. Here, the features of the microstructure of shungite were not taken into account.

At the upper boundary of the layer (on which the electromagnetic wave is incident), the components of the electric and magnetic fields are,

$$E_y^+ = E_i(1 + R),$$

$$H_x^+ = \frac{E_i}{Z_0}(1 - R),$$

where E_i is the complex amplitude of the electric field of the incident wave, Z_0 is the impedance of free space.

Under the lower boundary of the layer (with which the wave exits), the field components are,

$$E_y^- = E_i T,$$

$$H_x^- = \frac{E_i}{Z_0} T.$$

If we substitute of electromagnetic field components (6) and (7) into the approximate boundary conditions for a thin conducting layer obtained by the averaging method [29],

$$E_{x,y}^+ - E_{x,y}^- = \mp i\omega\mu d \cdot \frac{H_{y,x}^+ + H_{y,x}^-}{2},$$

$$H_{x,y}^+ - H_{x,y}^- = \pm \sigma(C) \cdot d \cdot \frac{E_{y,x}^+ + E_{y,x}^-}{2},$$

where $\mu = \mu_r \mu_0$ is magnetic permeability of the conducting layer, $\omega = 2\pi f$ is the cyclic frequency of the electromagnetic wave $f = 31$ GHz, then we find equations for the reflected and transmitted coefficient (power) [29,30] are,

$$R = \left| \frac{a - \beta}{(a + 1)(\beta + 1)} \right|^2,$$

$$T = \left| \frac{1 - a\beta}{(a + 1)(\beta + 1)} \right|^2,$$

The coefficients are defined by,

$$\alpha = \frac{i\omega\mu d}{2Z_0}$$

$$\beta = \frac{\sigma(C)dZ_0}{2}$$

The absorption power coefficient A reads as:

$$A = 1 - R - T$$

In our experiment, the coefficient $\alpha \ll \beta$ already with static conductivity of shungite ~ 100 S/m (for samples with a carbon concentration of $C > 17$ at.%), and it can be reduced. Then equations (10) and (11) can be simplified:

$$R = \left| \left(1 + \frac{2}{\sigma(C)Z_0 d} \right)^{-1} \right|^2,$$

$$T = \left| \frac{2}{\sigma(C)Z_0 d + 2} \right|^2$$

Fig. 6c shows the theoretical dependence of the absorption coefficient on the carbon concentration. The theoretical values were calculated using equation (10) – (14), where the experimental parameters were used in the coefficients (12)–(13): $f = 31$ GHz; d is the thickness of each shungite samples; $\sigma(C)$ is the conductivity of the sample at the corresponding carbon concentration (Table 1). In Fig. 6a and b the

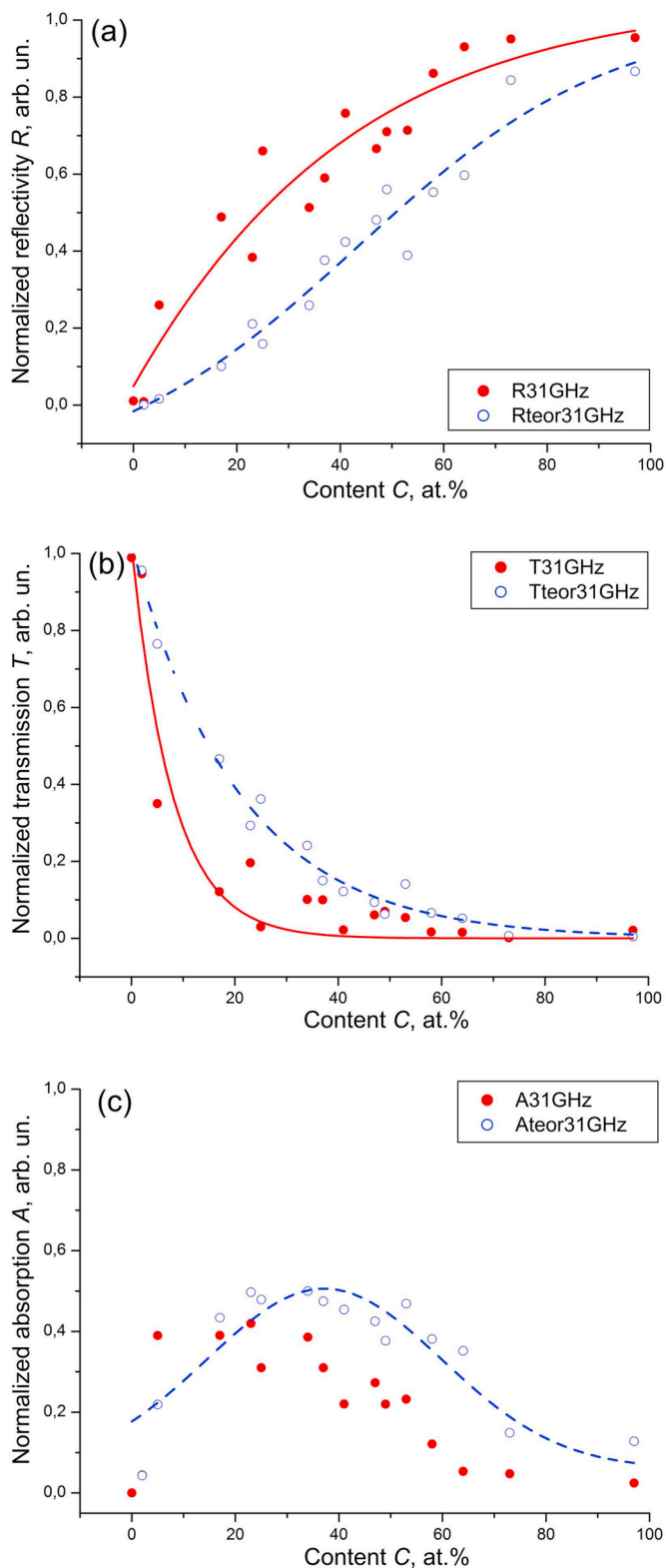


Fig. 6. Calculated reflection (a), transmission (b) and absorption (c) curves based on Maxwell equations versus experimental curves. Dotted lines and empty points are calculated, solid lines and solid points are experimental.

theoretical and experimental dependences of the reflection and transmission coefficients on carbon concentration are compared.

Theoretical dependences are approximated by functions (4) and (5), where for (4): $y(x) = R(C)$; $A_1 = -0.20$; $A_2 = 1.00$; $x_0 = 43.14$; $dx = 24.78$; and for (5): $y(x) = T(C)$; $y_0 = 0$; $B = 1.00$; $t = 20.91$.

As can be seen from Fig. 6c, the points in the theoretical dependence of absorption are rather well positioned along the Gaussian curve. Maximum occurs at $C \sim 34$ at.%, in which the shungite plate absorbs 50% of the entire incident microwave energy ($A = 0.5$).

The qualitative form of the theoretical dependence of the absorption does not coincide with the experimental one (Fig. 5c). Experimental points form a “plateau” in the concentration range $C \sim 5$ –34 at.%, where the absorption coefficient varies slightly around the mean value $A = 0.40 \pm 0.02$. When $C > 34$ at.%, experimental values of A monotonously decrease, similarly to theoretical ones; however, their difference is very noticeable and can be ~ 0.1 –0.3.

Fig. 6a shows that the predicted reflection is substantially less than the experimental one. For the two most high carbon samples, the theoretical and experimental transmission values are comparable, and the smallest difference in reflection values occurs. This is probably due to the greatest fit to the approximation of structure homogeneity for these samples. With decreasing carbon content, the gap between theoretical and experimental values increases, due to the fact that the complex microstructure of the samples includes additional mechanisms of reflection and absorption [1].

The depth of skin effect for studied samples was calculated. We estimated the dynamic conductivity of the shungite plate σ_D by the measured reflection coefficient within the framework of the approximation of a homogeneous structure by equation (15) [26]:

$$\sigma_D = \left[\frac{d Z_0}{2} \left(\frac{1}{\sqrt{R}} - 1 \right) \right]^{-1} \tag{17}$$

Here R is the experimental values of the reflection coefficient measured at a frequency of 31 GHz and presented in Fig. 5a.

We estimated the depth of skin effect δ by the equation:

$$\delta = \left(\frac{2}{\omega \cdot \mu \cdot \sigma} \right)^{1/2} \tag{18}$$

The results are shown in Table 2.

The electromagnetic interference shielding effectiveness is 90–95% (or about 20–25 dB) at carbon content of 17–37 at.%, and it is 96–100% (or within 30–60 dB) at carbon content of 41–97 at.%, (Table 2).

The calculation shows that the depth of the skin effect is comparable to the thickness of shungite plates with the carbon content of over 64%, and several times greater than shungite plate’s thickness with lower carbon contents. Thus, the interaction of incident radiation with matter occurs throughout the depth of the plate, and the discussion of reflection and absorption effects must be carried out taking into account the microstructure of shungite and the structure of shungite carbon.

Table 2

The experimental reflection coefficient (R_{exp}), static (σ_s) and dynamic (σ_D) conductivity, the depth of skin effect measured at static (δ_s) and dynamic (δ) conductivity, and shielding effectiveness coefficient ($R + A$).

Sample code	R_{exp} , arb. un.	σ_s , S/m	σ_D , S/m	δ_s , μm	δ , μm	$R + A$, arb. un.
ShSh1	0.954	6000	18680	37	21	0.989
ShSh2	0.951	4000	13910	45	24	1.0
ShL2	0.931	1500	12060	74	26	0.981
M59	0.862	1100	4910	86	41	0.982
M58	0.714	1100	3610	86	48	0.935
ShL2a	0.710	1050	1890	88	66	0.965
ShZ3	0.666	1000	1960	90	65	0.942
ShM3	0.758	900	3250	95	50	0.981
ShKG3	0.590	600	1260	117	81	0.905
ShCh3	0.513	500	1220	128	82	0.903
M29	0.660	270	1770	174	68	0.982
M30	0.384	300	580	165	119	0.948
M25	0.488	190	950	207	93	0.878
ShSh5	0.260	40	290	452	168	0.759
ShN5	0.009	8	40	1011	477	0.05

3.4. Influence of effective thickness on absorption of electromagnetic radiation by shungites

The concept of the effective layer d_{eff} [31] to take into account the effect of plate thickness on the dependence of reflection and absorption coefficients on concentration was used. We mean such a virtual layer in shungite plate, which would contain all the carbon from the plate, i.e:

$$d_{eff} = d \cdot \frac{C}{100}, \quad (19)$$

where C is the carbon content (atomic %); d is shungite plate thickness.

The dynamic conductivity was calculated depending on the effective thickness of the carbon layer by equation (14) using d_{eff} instead d . Linear dependencies for each deposit depending on carbon content were obtained (Fig. 7). In terms of their contribution to reflection, the effective microwave conductivity corresponds qualitatively to the static conductivity that is characteristic of samples from each deposit. The static conductivity of pure carbon from the Shunga deposit is 6000–8000 S/m, from Maxovo is about 2500 S/m, from Chebolaksha is about 2000 S/m, from Nigozero is about 1500 S/m [32,33]. This result shows that the scatter of points on the reflection/absorption curves may be due to the difference in the intrinsic conductivity of carbon in each deposit.

The jump of the microwave conductivity of the effective layer occurs when the carbon content is between 57 and 64%. Probably, the effect of the shungite microstructure on microwave properties at this concentration dramatically increases. At higher carbon contents, the contribution from reflection clearly dominates (Fig. 6). Since the carbon structure is the uniform at all carbon contents, below this interval, the mineral part of shungite strongly affects the microwave properties.

4. Discussion

Shielding carbon-containing materials is usually constructed on a non-conductive basis with conductive filler, which are nanotubes, fullerenes, soot particles, etc. The shielding effectiveness increases with the static conductivity. Below the percolation threshold, the shielding effectiveness slightly increases with the conductivity since in this case a small change in carbon filler content abruptly increases the conductivity while the effect on the shielding effectiveness is insignificant. After the percolation threshold, a small change in static conductivity causes a large increase in shielding effectiveness because, at this stage the shielding properties become significantly sensitive to a small change in conductivity [1]. The materials with graphene filler, which is one of the

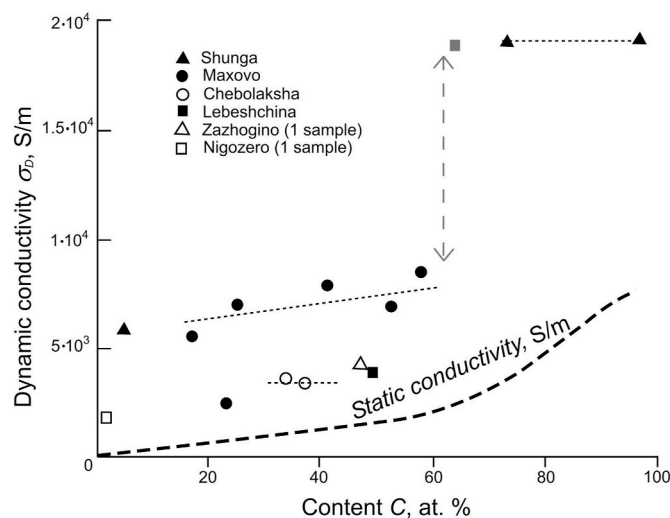


Fig. 7. The dynamic conductivity for the effective thickness d_{eff} of the carbon layer in shungite plates vs carbon content.

most effective, are the closest to shungite in the structure of the carbon filler.

In the studied natural system, glass-like carbon is a matrix in which the non-conducting phase is included as filler. This is a fundamental difference from the above described shielding systems, which allows, with a smaller thickness of the coatings and with lower carbon content, to achieve a large shielding efficiency, including absorption. Even with low carbon content, shungite plates show high efficiency of reflection and absorption. With an increase in carbon content, reflective properties begin to dominate, and the shielding efficiency tends to 100%.

Penographytitic and foamed materials are used to increase absorption because porosity of the material plays an important role in the absorption of electromagnetic radiation [2]. Shungite carbon has nanoscale porosity [34], which can improve absorption. Additionally, the multilayer stacked graphene exhibits increased absorption due to the total sheet resistance [35]. However, microscale inclusions of non-conducting minerals (primarily quartz) probably play the main role in absorption (Fig. 8).

The almost uniform distribution of quartz among carbon is due to the peculiarities of the geological origin of this rock. We call this phenomenon “sand impregnated with liquid” [26]. During the shungites formation the rock consisting mainly of quartz with the inclusions of pyrite, chalcopyrite and some other minerals was uniformly saturated with a hydrocarbon fluid. This fluid was formed from the original carbonaceous matter (presumably algae) under the influence of heat and (possibly) pressures during volcanic activity in the area about 2 billion years ago. The carbon content in a rock is mainly determined by its porosity. “Pure” shungite carbon was formed in large cracks and caverns. In Fig. 9, we present a very simplified (artificially averaged) model of the distribution of quartz in shungite.

The comparison of theoretical and experimental absorption coefficients shows that with a carbon content of over 35%, the approximating experimental curve is qualitatively similar to the theoretical one. In this case, the curves differ in absolute values. The theoretical absorption is substantially more than that obtained in the experiment. It is likely that substantially lower reflection efficiency was expected for samples in this range of carbon contents. For large carbon content, for our samples, the Maxwell approximation is correct, since the sizes of non-conductive inclusions are small and shungite plates can be considered as a pure carbon. Despite this, the experimental reflection values significantly exceed those expected for the measured values of conductivity. Experimental reflection from high carbon shungite exceeds reflection from metal films of comparable thickness [27,30]. Previously, multiple excess of the shielding effectiveness was found for a multi-layer graphene compared to the films of gold at the nanoscale [36]. In theoretical calculations, we did not take into account the microstructure of the shungite plate (Figs. 8 and 9). We believed that an electromagnetic wave fell on a chemically and structurally homogeneous plate. Equation (13) was applied for shungites in Ref. [26], which was obtained using the intragranular current model, according to which the behavior of the reflection coefficient for cubic granules is determined by the conductivity of the granules (conducting regions) σ_g , sample thickness d , granule sizes g and distances between them p [37]:

$$R = \left[\frac{\exp(-p/g) g Z_0}{\left(Z_0 + \frac{2(g+p)}{\sigma_g d g} \right) (g+p)} \right]^2 \quad (20)$$

The relation (13) can be obtained from (20) by performing an approximation for dimensions, i.e. the use of the averaging method in experimental conditions is fully justified.

However, for samples with carbon content below 35%, both qualitative and quantitative deviations from the theoretical curve occur. This suggests that in this range of contents, additional absorption and reflection mechanisms begin to play a key role. These mechanisms are

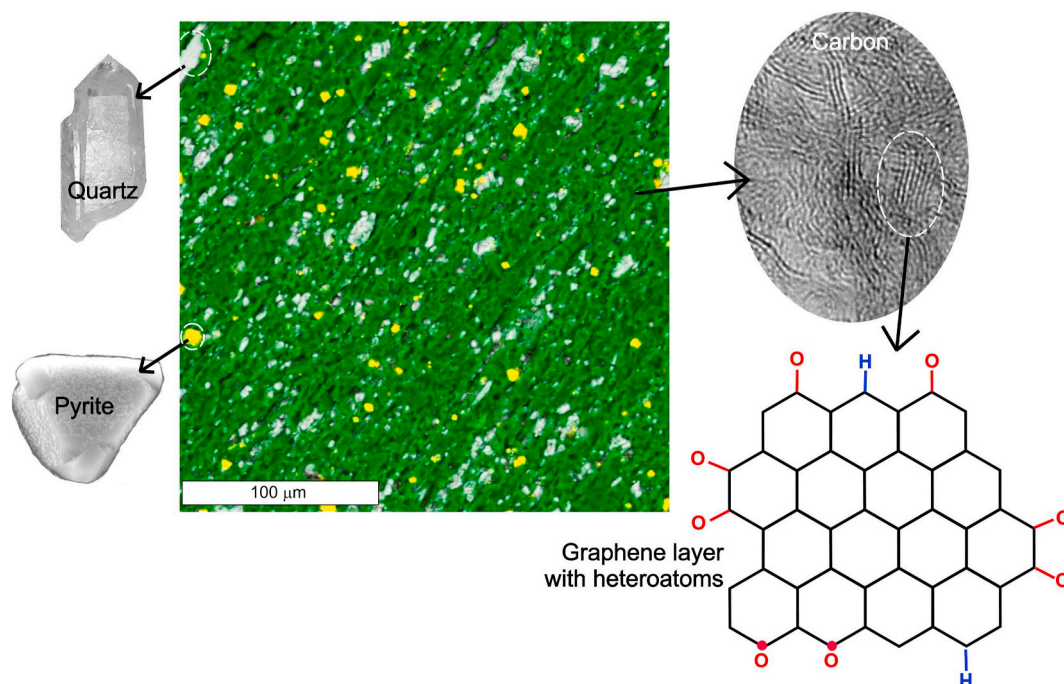


Fig. 8. Typical microstructure of shungite with medium carbon content. Inserts show basic mineral inclusions (quartz and pyrite) as well as the structure of shungite carbon.

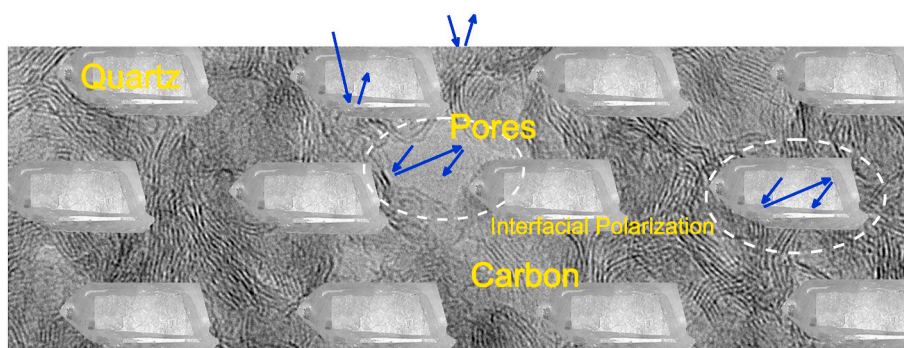


Fig. 9. Schematic representation of quartz-carbon composite microstructure of shungite and typical graphene-containing structure of shungite carbon.

not described by Maxwell equations for homogeneous systems, and they are associated with the microstructure of shungites [26].

The molecular graphene-containing structure of shungite carbon affects the reflection efficiency, which is superior to the reflection efficiency from metals with a conductivity that is orders of magnitude higher than that of shungite. The microstructure of shungite controls absorbing properties. In order for the reflection from high-carbon samples to match the calculated reflection (Fig. 6), their static conductivity must be significantly (several times) higher than the conductivity measured in the experiment. However, both our results of measurements of static conductivity, and the results of other authors [32,33], show that the conductivity of the pure carbon of shungite rocks of Karelia varies within 1500–8000 S/m. Therefore, even if we take the maximum value of conductivity, we will not get the required microwave conductivity to match Maxwell theory.

The representation of the shungite structure as a two-phase system “conducting carbon regions – non-conducting mineral regions” [26] made it possible to use the model of intragranular currents described for thin composite films in Ref. [37] to understand the reflection mechanism. This model is based on the currents circulation within the conductive components of the structure. An incident electromagnetic

wave in microwave conductive regions produces localized microwave currents that create magnetic fields of the same frequency, and these fields can be considered a source of secondary waves. Due to the currents circulating in the conducting regions, the wave is re-emitted by these regions. The re-radiation occurs in both directions relative to the surface, therefore the reflected and transmitted waves are formed. Thus, isolated conductive regions increase the reflection coefficient of microwave radiation. When the size of such conductive regions increases, the reflection becomes stronger.

Most of the experimental results indicate that the carbonaceous material must be doped on the surface with magnetic particles to have a strong absorption. Shungites already contain nanoscale inclusions and clusters of iron-containing particles with magnetic properties, in addition, shungite carbon structures have diamagnetism properties [9].

In addition, the absorption properties of the material are improved even with a small content of heteroatoms (H, O, N, S). Heteroatoms produce polarization centers and enhance absorption properties [38–41]. Shungite carbon contains several (2–4) percent of heteroatoms in the carbon structure [10,42], which are predominantly localized at the edges of stacks of graphene layers (Fig. 8). These residues of oxygen-containing functional groups and defects in the graphene

networks can act as dipolar centers, creating dipolar polarization [40, 41].

Thus, the main mechanisms of reflection in shungites are associated with stacks and ribbons of graphene layers with high conductivity, the main factors of absorption are the porous structure of carbon itself and non-conductive or weakly conductive mineral inclusions with dimensions of the first micrometers covered with graphene carbon layers. Since the porosity of high-carbon and medium-carbon samples is comparable, we think that the main absorption mechanism in shungites is the multiple interfacial polarization at the interface of phase with different dielectric constants, such as mineral inclusions/shells from graphene layers and pores in the carbon structure. This does not contradict the estimates that interphase polarization should be one of the main mechanisms of relaxation weakening at frequencies of several tens of GHz [38].

The results of this study show that the production of shielding and absorbing materials based on conductive carbon matrices with non-conductive filler contributes to obtaining substantially thinner coatings with comparable shielding effectiveness. Some applications require obtaining very thin (first tens of micrometers) and flexible shielding and absorbing materials. It is therefore important to study of composite systems similar to natural shungites. In this work, thin plates of natural shungite have been fabricated, completely preserving their original microstructure and applied properties (strength and durability, high chemical stability and fire resistance). A thickness of 10–20 μm and an electromagnetically transparent substrate allows the plates to be very flexible and retain their protective properties under many bends. Thus, it becomes possible to combine reflective and absorbing properties by selecting raw material with different carbon content. To achieve such shielding effectiveness, materials with a thickness of several millimeters are now mainly used. Shungites can be considered as a raw material for the manufacture of shielding materials, and as a model system for studying the interaction of electromagnetic radiation with a substance, the microstructure of which can be described as “sand impregnated with liquid” with a carbon conducting matrix.

Natural materials are interesting because the synthesis of such materials is difficult. In nature, the processes of their formation take millions of years, and almost all chemical reactions are completed. There is no such amount of time in the laboratory; it is necessary to use catalysts to speed up chemical reactions. This leads to possible changes in the structure of the material and additional costs for the search of catalysts.

5. Conclusion

Flexible ultrathin (with a thickness of 10–20 μm) shielding plates with a wide variation of the reflection and absorption effectiveness of microwave radiation were successfully prepared by polishing from natural graphene-containing shungites. The reflection coefficient of shungites with an increase in carbon content from 2 to 40–50 at. % is dramatically increased from almost zero to 0.8. With a further increase in carbon content, the reflection coefficient grows weakly, down to about one at $C = 64\%$. For successful reflection of microwave radiation, the use of shungites with carbon content in the range of 64–95% is optimal. For shielding with the absorption of a significant part of the radiation, the optimum range of carbon contents is 5–34%. Absorption is most effective when the plate thickness is in the range of about 10–20 μm . When the plate thickness increases to 100 μm , the reflection effectiveness increases to 100% even at a low carbon content (about 5%). The molecular structure determines the reflective properties of shungite carbon that are superior to the reflective properties of high-conductivity metals. The microstructure controls absorption ability of shungite. Thus, shungites, as natural graphene-containing carbon, are classic green materials for effective protection from microwave radiation. The advantage of shungite plates as shielding materials is their low cost, thermal and chemical resistance, very small thickness (10–20 μm), flexibility and lightweight, high absorption coefficient along with a high

reflection coefficient at different carbon content. The research results show that the development of shielding systems, based on conductive carbon matrices with the introduction of non-conductive filler, can improve the efficiency of shielding, especially absorption, at small thicknesses of such systems.

Declaration of competing interest

The authors declare that they have no known competing financial interests or personal relationships that could have appeared to influence the work reported in this paper.

Acknowledgements

The reported study was funded by RFBR and NSFC according to the research project RFBR N^o 20-55-53019 and NSFC N^o 42011530085. The authors thank Dr. Roman V. Sadovnichy (Institute of Geology of Karelian SC of RAS, Petrozavodsk) for some samples (with “M” as the first symbol in their code) and Alexandr A. Utkin for the scanning electron microscopy assistance.

References

- [1] J.M. Thomassin, C. Jerome, T. Pardoën, C. Bailly, I. Huynen, C. Detrembleur, Polymer/carbon based composites as electromagnetic interference (EMI) shielding materials, *Mater. Sci. Eng. R* 74 (2013) 211–232, <https://doi.org/10.1016/j.mser.2013.06.001>.
- [2] I. Huynen, N. Quievie, C. Bailly, P. Bollen, C. Detrembleur, S. Eggermont, I. Molenberg, J.M. Thomassin, L. Urbanczyk, T. Pardoën, Multifunctional hybrids for electromagnetic absorption, *Acta Mater.* 59 (2011) 3255–3266, <https://doi.org/10.1016/j.actamat.2011.01.065>.
- [3] F. Qin, C. Brosseau, A review and analysis of microwave absorption in polymer composites filled with carbonaceous particles, *J. Appl. Phys.* 111 (2012), 061301, <https://doi.org/10.1063/1.3688435>.
- [4] D.D.L. Chung, Electromagnetic interference shielding effectiveness of carbon materials, *Carbon* 39 (2001) 279–285, [https://doi.org/10.1016/S0008-6223\(00\)00184-6](https://doi.org/10.1016/S0008-6223(00)00184-6).
- [5] D.D.L. Chung, Carbon materials for structural self-sensing, electromagnetic shielding and thermal interfacing, *Carbon* 50 (2012) 3342–3353, <https://doi.org/10.1016/j.carbon.2012.01.031>.
- [6] J. Liang, Y. Wang, Y. Huang, Y. Ma, Z. Liu, J. Cai, C. Zhang, H. Gao, Y. Chen, Electromagnetic interference shielding of graphene/epoxy composites, *Carbon* 47 (2009) 922–925, <https://doi.org/10.1016/j.carbon.2008.12.038>.
- [7] V.A. Melezchik, M.M. Filippov, A.E. Romashkin, A giant paleoproterozoic deposit of shungite in NW Russia, *Ore Geol. Rev.* 24 (2004) 135–154.
- [8] V.I. Berezkin, S.V. Kholodkevich, P.P. Konstantinov, Hall effect in the natural glassy carbon of shungites, *Phys. Solid State* 39 (1997) 1590–1593, <https://doi.org/10.1134/1.1129903>.
- [9] V.V. Kovalevski, A.V. Prikhodko, P.R. Buseck, Diamagnetism of natural fullerene-like carbon, *Carbon* 43 (2005) 401–405, <https://doi.org/10.1016/j.carbon.2004.09.030>.
- [10] E.A. Golubev, Electrophysical properties and structural features of shungite (natural nanostructured carbon), *Phys. Solid State* 55 (2013) 1078–1086, <https://doi.org/10.1134/S1063783413050107>.
- [11] N.H. Chou, N. Pierce, Y. Lei, N. Perea-López, K. Fujisawa, S. Subramanian, J. A. Robinson, G. Chen, K. Omichi, S.S. Rozhkov, N.N. Rozhkova, M. Terrones, A. R. Harutyunyan, Carbon-rich shungite as a natural resource for efficient Li-ion battery electrodes, *Carbon* 130 (2018) 105–111.
- [12] E. Tamburri, R. Carcione, S. Politi, M. Angiellari, L. Lazzarini, L.E. Vanzetti, S. Macis, G. Peponi, M.L. Terranova, Shungite carbon as unexpected natural source of few-layer graphene platelets in a low oxidation state, *Inorg. Chem.* 57 (2018) 8487–8498, <https://doi.org/10.1021/acs.inorgchem.8b01164>.
- [13] R. Gusmao, Z. Sofer, D. Bouša, M. Pumera, Synergetic metals on carbocatalyst shungite, *Chem. Eur. J.* 23 (2017) 18232–18238, <https://doi.org/10.1002/chem.201703974>.
- [14] P.R. Buseck, L.P. Galdobina, V.V. Kovalevski, N.N. Rozhkova, J.W. Valley, A. Z. Zaidenberg, Shungites: the C-rich rocks of Karelia, Russia, *Can. Mineral.* 35 (1997) 1363–1378.
- [15] B. Kwiecinska, Investigations of shungite, *Bull. Polish Acad. Sci. (Chem.)* 16 (1968) 61–65.
- [16] P.R. Buseck, B.J. Huang, Conversion of carbonaceous material to graphite during metamorphism, *Geochem. Cosmochim. Acta* 49 (1985) 2003–2016, [https://doi.org/10.1016/0016-7037\(85\)90059-6](https://doi.org/10.1016/0016-7037(85)90059-6).
- [17] YuK. Kalinin, K.U. Usenbaev, V.V. Kovalevskii, Shungite Structure as a Function of the Conditions of its Formation, *Mineralogy and Geochemistry of the Precambrian of Karelia*, IG Kar SC RAS, Petrozavodsk, 1979, pp. 111–123 (in Russian).
- [18] E.F. Sheka, N.N. Rozhkova, Shungite as loosely packed fractal nets of graphenebased quantum dots, *Int. J. Smart Nano Mat.* 5 (1) (2014) 1–16.

- [19] E.F. Sheka, E.A. Golubev, Technical graphene (reduced graphene oxide) and its natural analog (shungite), *Tech. Phys.* 61 (2016) 1032–1038, <https://doi.org/10.1134/S1063784216070239>.
- [20] T.G. Shumilova, *Mineralogy of Native Carbon*, UrO RAS Press, Ekaterinburg, 2002 (in Russian).
- [21] V.V. Kovalevski, P.R. Buseck, J.M. Cowley, Comparison of carbon in shungite rocks to other natural carbons: an X-ray and TEM study, *Carbon* 39 (2001) 243–256, [https://doi.org/10.1016/S0008-6223\(00\)00120-2](https://doi.org/10.1016/S0008-6223(00)00120-2).
- [22] L.M. Lyn'kov, T.V. Borbot'ko, E.A. Krishtopova, Radio-absorbing properties of nickel-containing shungite powder, *Tech. Phys. Lett.* 35 (2009) 410–411, <https://doi.org/10.1134/S1063785009050071>.
- [23] I.A. Moshnikov, V.V. Kovalevski, Electrophysical properties of shungites at low temperatures, *Nanosyst. Phys. Chem. Math.* 1 (2016) 214–219, <https://doi.org/10.17586/2220-8054-2016-7-1-214-219>.
- [24] S. Emelyanov, A. Kuzmenko, V. Rodionov, M. Dobromyslov, Mechanisms of Microwave Absorption in carbon compounds from shungite, *J. Nano Electron. Phys.* 5 (3pp) (2013), 04023.
- [25] YeA. Golubev, I.V. Antonets, Influence of mineralogical and petrographic features on microwave radiation reflection from shungite rocks in the range 26–39 GHz, *Vestnik IG Komi SC UB RAS* 5 (2017) 43–48, <https://doi.org/10.19110/2221-1381-2017-5-43-48> (in Russian).
- [26] YeA. Golubev, I.V. Antonets, V.I. Shcheglov, Static and dynamic conductivity of nanostructured carbonaceous shungite geomaterials, *Mater. Chem. Phys.* 226 (2019) 195–203, <https://doi.org/10.1016/j.matchemphys.2019.01.033>.
- [27] I.V. Antonets, L.N. Kotov, S.V. Nekipelov, YeA. Golubev, Nanostructure and conductivity of thin metal films, *Tech. Phys.* 49 (3) (2004) 306–309, <https://doi.org/10.1134/1.1688415>.
- [28] D.Ya Khaliullin, S.A. Tret'yakov, Generalized impedance-type boundary conditions for thin planar layers of various media (review), *J. Commun. Technol. Electron.* 43 (1998) 12–25.
- [29] I.V. Antonets, *The Reflective and Conductive Properties of Thin Metal Films and Their Nanostructure*, SSU Press, Syktyvkar, 2007 (in Russian).
- [30] I.V. Antonets, L.N. Kotov, S.V. Nekipelov, E.N. Karpushov, Conducting and reflecting properties of thin metal films, *Tech. Phys.* 49 (2004) 1496–1500, <https://doi.org/10.1134/1.1826197>.
- [31] I.V. Antonets, L.N. Kotov, YeA. Golubev, Influence of composition and nanogranular structure of (Co+Fe+Zr)/(ZrO) composite films on conductivity and microwave reflective properties, *Mater. Chem. Phys.* 240 (2020) 122097, <https://doi.org/10.1016/j.matchemphys.2019.122097>.
- [32] YuK. Kalinin, A.P. Punka, Electrical conductivity, in: V.A. Sokolov, YuK. Kalinin, E. F. Dyukkiev (Eds.), *Shungites – New Carbon Raw Materials*, Petrozavodsk, Karelia, 1984, pp. 53–59 (in Russian).
- [33] M.A. Augustyniak-Jabłokow, Y.V. Yablokov, B. Andrzejewski, W. Kempirski, S. Łoś, K. Tadzyszak, M.Y. Yablokov, V.A. Zhikharev, EPR and magnetism of the nanostructured natural carbonaceous material shungite, *Phys. Chem. Miner.* 37 (2010) 237–247, <https://doi.org/10.1007/s00269-009-0328-9>.
- [34] YeA. Golubev, V.V. Ulyashev, A.A. Veligzhanin, Porosity and structural parameters of Karelian shungites according to the data of small-angle synchrotron radiation scattering and microscopy, *Crystallogr. Rep.* 61 (1) (2016) 66–77, <https://doi.org/10.1134/S1063774516010077>.
- [35] B. Wu, H.M. Tuncer, A. Katsounaros, W. Wu, M.T. Cole, K. Ying, Y. Hao, Microwave absorption and radiation from large-area multilayer CVD graphene, *Carbon* 77 (2014) 814–822, <https://doi.org/10.1016/j.carbon.2014.05.086>.
- [36] S.K. Hong, K.Y. Kim, T.Y. Kim, J.H. Kim, S.W. Park, J.H. Kim, B.J. Cho, Electromagnetic interference shielding effectiveness of monolayer graphene, *Nanotechnology* 23 (45) (2012) 455704.
- [37] I.V. Antonets, L.N. Kotov, O.A. Kirpicheva, E.A. Golubev, Y.E. Kalinin, A. V. Sitnikov, V.G. Shavrov, V.I. Shcheglov, Static and dynamic conduction of amorphous nanogranulated metal–dielectric composites, *J. Commun. Technol. Electron.* 60 (2015) 904–914, <https://doi.org/10.7868/S0033849415070013>.
- [38] H. Zhao, Y. Cheng, W. Liu, L. Yang, B. Zhang, L.P. Wang, G. Ji, Z.J. Xu, Biomass-derived porous carbon-based nanostructures for microwave absorption, *Nano-Micro Lett.* 11 (2019) 24, <https://doi.org/10.1007/s40820-019-0255-3>.
- [39] Y. Cheng, J.Z.Y. Seow, H. Zhao, Z.J. Xu, G. Ji, A flexible and lightweight biomass-reinforced microwave absorber, *Nano-Micro Lett.* 12 (2020) 125, <https://doi.org/10.1007/s40820-020-00461-x>.
- [40] X. Liang, Z. Man, B. Quan, J. Zheng, W. Gu, Z. Zhang, G. Ji, Environment-stable CoxNiy encapsulation in stacked porous carbon nanosheets for enhanced microwave absorption, *Nano-Micro Lett.* 12 (2020) 102, <https://doi.org/10.1007/s40820-020-00432-2>.
- [41] L. Wang, M. Huang, X. Yu, W. You, J. Zhang, X. Liu, M. Wang, R. Che, MOF-derived Ni1–xCox@Carbon with tunable nano–microstructure as lightweight and highly efficient electromagnetic wave absorber, *Nano-Micro Lett.* 12 (2020) 102, <https://doi.org/10.1007/s40820-020-00488-0>.
- [42] YeA. Golubev, N.N. Rozhkova, YeN. Kabachkov, YuM. Shul'ga, K. Natkaniec-Holdera, I. Natkaniec, I.V. Antonets, B.A. Makeev, N.A. Popova, V.A. Popova, E. F. Sheka, sp² amorphous carbons in view of multianalytical consideration: normal, expected and new, *J. Non-Cryst. Solids* 524 (2019) 119608, <https://doi.org/10.1016/j.jnoncrsol.2019.119608>.